

Guided modes in graphene waveguides

Fan-Ming Zhang¹, Ying He¹, and Xi Chen^{1,2*}

¹ *Department of Physics, Shanghai University, 200444 Shanghai, People's Republic of China and*

² *Departamento de Química-Física, UPV-EHU, Apdo 644, 48080 Bilbao, Spain*

(Dated: January 15, 2025)

By analogy of optical waveguides, we investigate the guided modes in graphene waveguides, which is made of symmetric quantum well. The unique properties of the graphene waveguide are discussed based on the two different dispersion relations, which correspond to classical motion and Klein tunneling, respectively. It is shown that the third-order mode is absent in the classical motion, while the fundamental mode is absent in the Klein tunneling case. We hope these phenomena can lead to the potential applications in graphene-based quantum devices.

PACS numbers: 81.05.Uw, 73.63.-b, 78.20.Ci, 42.82.Et

There has been great interest in the investigations of graphene [1–3], since the two-dimensional form of carbon named graphene was realized experimentally by A. Geim *et al.* in 2004 [4]. This material is densely packed into a honeycomb structure, which is made out of two distinct triangular sublattices, is labeled by A and B. The low energy band structure of graphene is gapless, with massless chiral carriers. These unusual structure is thus the root of special phenomenon such as anomalous quantum Hall effect [5–7], minimum conductivity [5, 6], and Klein tunneling [2, 8]. It is also interesting that the Klein paradox describes a phenomenon that the relativistic electron can pass through a high barrier perfectly in contrast to the conventional tunneling. These phenomena are expected to play an important role in the future nanoelectronic devices.

It is well established that electronic analogies of many optical behaviors have been achieved in two-dimensional electron gas (2DEG) system [9, 10]. Since the mean-free path approaches to the order of micron at room temperature, ballistic electrons behave the quantum wave nature of electron, that is, electrons can refract, reflect, and interfere in a manner analogous to electromagnetic waves in dielectrics [11–13]. Furthermore, electron waveguides [14–20] have also been extensively demonstrated theoretically and experimentally. Very recently, graphene opens a way to study different optics-like phenomena [21–26], such as negative refraction [21], Goos-Hänchen effect [24], Bragg reflection [25], and graphene waveguide [26].

In this Letter, we investigate the guided modes in graphene quantum well (QW) [27], acting as a slab waveguide for electron waves in a form similar to integrated optics. As a matter of fact, the waveguide configuration of graphene p-n-p junction considered here can be tailored to desired form and size. For example, a gate-tunable graphene device can be fabricated from a single-layer graphene sheet, which is modulated by n^{++} Si substrate as the back gate and the Ti Au strip as the top

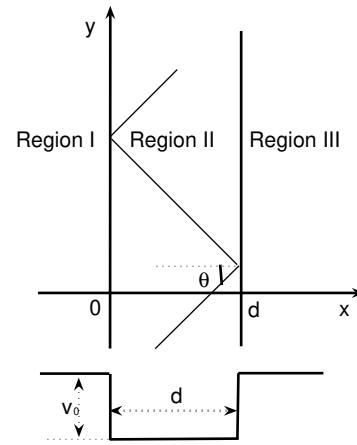


FIG. 1: Schematic diagram of the graphene waveguides.

gate. The carrier density in the bulk of the graphene sheet is tuned by a voltage applied to the back gate, and the density in the narrow strip below the top gate is tuned by a voltage applied to the top gate [28].

For simplicity, we consider a symmetric QW waveguide structure of monolayer graphene, as shown in Fig. 1, where the potential profile of the three zones are denoted by

$$V(x) = \begin{cases} V_0, & \text{otherwise,} \\ 0, & 0 \leq x \leq d. \end{cases} \quad (1)$$

The electron wave with angle θ known as the *zig-zag* angle respect to the x axis is incident to the QW, the direction of guided mode propagation is y axis, and there are two types of situations: (a) when the zigzag angle is less than the total internal reflection (TIR) angle, the modes become radiation modes; (b) if the incident angle is more than the critical angle, there will exist oscillating guided modes. What as follows we will focus on the latter case. The TIR angle is defined by $\sin \theta_c = \kappa_2 / \kappa_1$,

*Author to whom correspondence should be addressed; Email address: xchen@shu.edu.cn

where $\kappa_1 = |E|/\hbar v_F$, $\kappa_2 = |E - V_0|/\hbar v_F$ are wave vectors in region II and region III (or region I), E is the electron energy, \hbar is Planck's constant h divided by 2π , $v_F \approx 10^6 m/s$ is Fermi velocity. Carriers in graphene exhibit ballistic transport on the submicron scale, and are governed by the following Dirac-type equation:

$$H = -i\hbar v_F \sigma \nabla + V(x), \quad (2)$$

where $\sigma = (\sigma_x, \sigma_y)$ are the Pauli's matrices. The Hamiltonian acts on the states expressed by the two-component spinors $\Psi = [\Psi_A, \Psi_B]^T$, where Ψ_A, Ψ_B represent the smooth enveloping functions at the respective sublattice sites of graphene. Due to translation invariance in the y direction, we give the solution in the time-independent form $\Psi_m(x, y) = \psi_m(x)e^{i\kappa_y y}$, $m = A, B$, thus obtain

$$\begin{aligned} -i\hbar v_F \left(\frac{d\psi_B}{dx} + \kappa_y \psi_B \right) &= (E - V(x))\psi_A, \\ -i\hbar v_F \left(\frac{d\psi_A}{dx} - \kappa_y \psi_A \right) &= (E - V(x))\psi_B. \end{aligned} \quad (3)$$

The character of the spinors solution in the three regions can be written as:

$$\begin{aligned} \psi_A(x) &= \begin{cases} Ae^{\alpha x}, & x < 0, \\ B \cos(\kappa_x x) + C \sin(\kappa_x x), & 0 < x < d, \\ De^{-\alpha(x-d)}, & x > d, \end{cases} \\ \psi_B(x) &= \begin{cases} -iAs' \frac{\delta - \sin\theta}{\sin\theta_c} e^{\alpha x}, & x < 0, \\ is(B \sin(\kappa_x x + \theta) - C \cos(\kappa_x x + \theta)), & 0 < x < d, \\ is'D \frac{\delta + \sin\theta}{\sin\theta_c} e^{-\alpha(x-d)}, & x > d. \end{cases} \end{aligned} \quad (4)$$

We define $s = \text{sgn}(E)$, $s' = \text{sgn}(E - V_0)$, $\delta = \sqrt{\sin^2 \theta - \sin^2 \theta_c}$, $\kappa_x = \kappa_1 \cos \theta$, $\kappa_y = \kappa_1 \sin \theta$, and $\alpha = \sqrt{\kappa_1^2 \sin^2 \theta - \kappa_2^2}$ is the evanescent coefficient when condition $0 < V_0 < 2E$ is satisfied. Applying the continuity of wave function at the interfaces $x = 0$ and $x = d$, we obtain the corresponding dispersion equation as follows,

$$\tan(\kappa_x d) = \frac{ss' \cdot \kappa_x \sqrt{\kappa_y^2 - \kappa_2^2}}{\kappa_1 \kappa_2 - ss' \kappa_y^2}, \quad (5)$$

In order to describe the right-hand-side of Eq. (5) as a function of $\kappa_x d$ and reveal the guided modes, we make Eq. (5) in dimensionless form

$$F(\kappa_x d) = \frac{ss' \cdot (\kappa_x d) \sqrt{(\kappa_1 d)^2 - (\kappa_x d)^2 - (\kappa_2 d)^2}}{-ss' [(\kappa_1 d)^2 - (\kappa_x d)^2] + (\kappa_1 d) \times (\kappa_2 d)}. \quad (6)$$

The dispersion equation (5) is a transcendental one and cannot be solved analytically, so we propose a graphical method to determine the solution of $\kappa_x d$ for the guided modes. Due to the different ss' , we will discuss the properties of the guided modes in the following two cases, respectively.

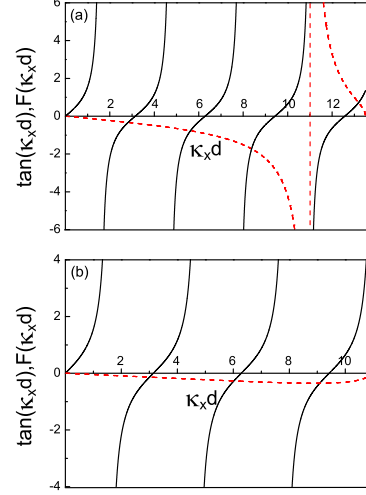


FIG. 2: Graphical determination of $\kappa_x d$ for oscillating guided modes, the solid and dashed curves correspond to the $\tan(\kappa_x d)$, $F(\kappa_x d)$ respectively, where physical parameters are chosen to be $U_0 = 50 meV$, (a) $\kappa_1 d = 4.96\pi$, $\kappa_2 d = 2.48\pi$, $ss' = 1$, and (b) $\kappa_1 d = 4\pi$, $\kappa_2 d = 2\pi$, $ss' = -1$.

i) When $ss' = 1$, we get one of the dispersion equations. The electron makes an intraband tunneling from an electron-like to another electron-like, which corresponds to the case of classical motion. To determine the guided modes, we plot the dependencies of $F(\kappa_x d)$ and $\tan(\kappa_x d)$ on $\kappa_x d$ in Fig. 2(a). The intersections show the existence of the guided modes. For the given parameters, we can get four $\kappa_x d$ from the graph directly. The profiles of waves function corresponding to the four guided modes are shown in Fig. 3.

As shown in Fig. 3, the states of ψ_A and $-i\psi_B$ have similar characteristic, we discuss only the wave function ψ_A . It is clearly seen that the electron waveguide supports fundamental mode, first-order mode, second-order mode and fourth-order mode, but the third-order mode is missing. In fact, the hierarchy of the guided modes is dependent on the incident energy. For a given QW electron waveguide, when the incident energy is not sufficiently large with respect to the critical angle for the third-order mode, this mode can not exist. It is seen that for greater incident energy, the third-order mode will also be vanished. In a word, the properties of the guided modes in the classical motion case are analogous to those in the conventional QW electron waveguide [12]. In addition, the tiny shift between the two wave function is also demonstrated, because the electron velocity of ψ_A and $-i\psi_B$ are different.

ii) If $ss' = -1$, another dispersion equation is obtained. The electron makes an intraband tunneling from an electron-like to hole-like, which corresponds to the case of Klein tunneling. In this case, the incident parti-

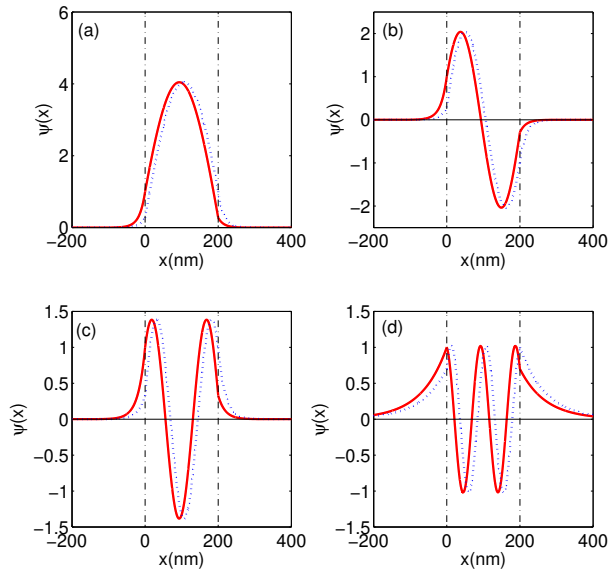


FIG. 3: The wave function of guided modes as function of distance of graphene waveguide corresponding to the intersections in Fig. 2(a). The solid curve and the dashed curve correspond to ψ_A and $-i\psi_B$, respectively. The physical parameters are $d = 200\text{nm}$, (a) $\kappa_x d = 2.82$, $\theta = 79.6^\circ$, (b) $\kappa_x d = 5.63$, $\theta = 68.8^\circ$, (c) $\kappa_x d = 8.38$, $\theta = 57.48^\circ$, (d) $\kappa_x d = 13.2$, and $\theta = 32.2^\circ$.

cles are predicted to tunnel through the symmetric potential barriers with unit probability when the incident energy $E < V_0$ is satisfied [8]. This manifests the combination of the conservation of the transverse momentum and the absence of backscattering. Similarly the intersections of dashed curves with solid curves indicate the existence of solutions for guided modes, as shown in Fig. 2 (b). Moreover, we could get the $\kappa_x d$ from the graph directly, and describe the wave function of the corresponding intersection in Fig. 4.

From Fig. 4 it is demonstrated that the number of the nodes of the guided modes ψ_A begins from one and is order-producing with the decreasing angle. In the case of Klein tunneling, the properties of the QW electron waveguides are found to be quite different. The conventional hierarchy of guided modes disappears. Specifically, the fundamental node-less mode does not exist at all, which is the particular property corresponding to the Klein tunneling in graphene QW waveguide, since the fundamental mode exists only when $E > V_0$ in the conventional QW electron waveguide. Fig. 4 manifests an obvious shift between the wave function ψ_A and $-i\psi_B$, which is due to the different speed between the electron for ψ_A and that of the hole for $-i\psi_B$. The wave function ψ_A shows a peak closing to the right interface between region II and region III, while the $-i\psi_B$ shows a peak closing to the left interface between region I and region

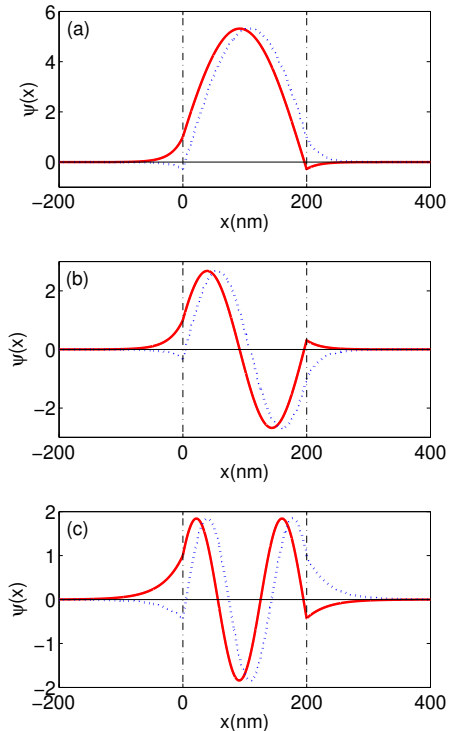


FIG. 4: The wave function of guided modes as function of distance of graphene waveguide corresponding to the intersections in Fig. 2 (b). The solid curve and the dashed curve correspond to ψ_A and $-i\psi_B$, respectively. The physical parameters are $d = 200\text{nm}$, (a) $\kappa_x d = 3.0$, $\theta = 76.2^\circ$, (b) $\kappa_x d = 6.02$, $\theta = 61.4^\circ$, (c) $\kappa_x d = 9.08$, $\theta = 43.7^\circ$.

II.

Finally, we should mention that when the graphene ribbons are narrow with the widths in the range of micrometer or submicrometer, the two types of edge states, which are current-carrying and dispersionless surface states [29], have strong influence on the transport of the quantum Hall region. However, it is shown in this paper that the oscillating guided modes guided by the electron wave have the strong energy flux localized inside the well region of graphene waveguides. In addition, the amplitude of the electron wave is oscillating in the well region and is evanescent out of the well. Thus, the influence of the edge states can be neglected in this problem.

In conclusion, we have investigated the guided modes in graphene waveguides. The oscillating guided modes of electron waves have features analogous to those of classical guided modes in ordinary dielectric structures. It is shown that the amplitude of electron wave function is oscillating in the well region and is evanescent out of the well. We obtain two different dispersion relations. In the classical case the absence of third-order mode is demon-

strated, while for the Klein tunneling case, the fundamental mode is absent. With the development of graphene, we hope that based on these electron wave propagation characteristics, a wide variety of graphene-based devices can be motivated by the application in the control and guiding of ballistic electrons in the future.

This work was supported in part by the National Natural Science Foundation of China (60806041, 60877055),

the Shanghai Rising-Star Program (08QA14030), the Science and Technology Commission of Shanghai Municipal (08JC14097), the Shanghai Educational Development Foundation (2007CG52), and the Shanghai Leading Academic Discipline Program (S30105). X. Chen is also supported by Juan de la Cierva Programme of Spanish Ministry of Science and Innovation.

-
- [1] A. H. Castro Neto, F. Guinea, N. M. R. Peres, K. S. Novoselov and A. K. Geim, *Rev. Mod. Phys.* **81**, 1 (2009).
- [2] C. W. Beenakker, *Rev. Mod. Phys.* **80**, 1337 (2008).
- [3] M. I. Katsnelson, *Mater. Today* **10**, 1 (2007).
- [4] K. S. Novoselov, A. K. Geim, S. V. Morozov, D. Jiang, Y. Zhang, S. V. Dubonos, I. V. Grigorieva, and A. A. Firsov, *Science* **306**, 666 (2004).
- [5] K. S. Novoselov, A. K. Geim, S. V. Morozov, D. Jiang, M. I. Katsnelson, I. V. Grigorieva, S. V. Dubonos, and A. A. Firsov, *Nature* **438**, 197 (2005).
- [6] Y. Zhang, Y. W. Tan, H. L. Stormer, and P. Kim, *Nature* **438**, 201 (2005).
- [7] V. P. Gusynin and S. G. Sharapov, *Phys. Rev. Lett.* **95**, 146801 (2005).
- [8] M. I. Katsnelson, K. S. Novoselov, and A. K. Geim, *Nature Phys.* **2**, 620 (2006).
- [9] S. Datta, *Electronic Transport in Mesoscopic Systems* (Cambridge University Press, New York, 1996), p. 276.
- [10] *Quantum-Classical Analogies*, edited by D. Dragoman and M. Dragoman (Springer, Berlin, 2004).
- [11] T. K. Gaylord, and K. F. Brennan, *J. Appl. Phys.* **65**, 814 (1989).
- [12] D. W. Wilson, E. N. Glytsis, and T. K. Gaylord, *IEEE J. Quantum Electron.* **29**, 1364 (1993).
- [13] A. Yacoby, M. Heiblum, V. Umansky, H. Shtrikman, and D. Mahalu, *Phys. Rev. Lett.* **73**, 3149 (1994).
- [14] T. K. Gaylord, E. N. Glytsis, and K. F. Brennan, *J. Appl. Phys.* **66**, 1842 (1989).
- [15] J. Q. Wang and B. Y. Gu, *Phys. Rev. B* **47**, 13442 (1993).
- [16] J. J. Palacios and C. Tejedor, *Phys. Rev. B* **48**, 5386 (1993).
- [17] R. Q. Yang, *J. Appl. Phys.* **80**, 1541 (1993).
- [18] T. N. Oder, J. Y. Lin, and H. X. Jiang, *Appl. Phys. Lett.* **79**, 2511 (2001).
- [19] T. H. Stievater, W. S. Rabinovich, D. Park, J. B. Khurgin, S. Kanakaraju, and C. J. K. Richardson. *Opt. Express* **16**, 2621 (2008).
- [20] C. C. Eugster, J. A. del Alamo, M. R. Melloch, and M. J. Rooks, *Phys. Rev. B* **48**, 15057 (1993).
- [21] V. V. Cheianov, V. Fal'ko, and B. L. Altshuler, *Science* **315**, 1252 (2007).
- [22] C. H. Park, Y. W. Son, L. Yang, M. L. Cohen, and S. G. Louie, *Nano Lett.* **8**, 2920 (2008).
- [23] P. Darancet, V. Olevano, and D. Mayou. *Phys. Rev. Lett.* **102**, 136803 (2009).
- [24] C. W. J. Beenakker, R. A. Sepkhanov, A. R. Akhmerov, and J. Tworzyd, *Phys. Rev. Lett.* **102**, 146804 (2009).
- [25] S. Ghosh, and M. Sharma, arXiv:0806.2951v4.
- [26] L. Zhao and S. F. Yelin, arXiv:0804.2225v2.
- [27] J. M. Pereira, Jr., V. Mlinar, F. M. Peeters, and P. Vasilopoulos, *Phys. Rev. B* **74**, 045424 (2006).
- [28] V. P. Gusynin and S. G. Sharapov, *Phys. Rev. Lett.* **98**, 286803 (2007).
- [29] L. Brey and H. A. Fertig, *Phys. Rev. B* **73**, 195408 (2006).